GEOPHYSICS, VOL. 87, NO. 5 (SEPTEMBER-OCTOBER 2022); P. V419–V435, 18 FIGS.
10.1190/GEO2021-0830.1

DOI:10.1190/geo2021-0830.1

Multiplicative random seismic noise caused by small-scale near-surface scattering and its transformation during stacking

Andrey Bakulin[1], Dmitry Neklyudov[2], and Ilya Silvestrov[1]

ABSTRACT

Even after sophisticated processing, land seismic data in complex areas exhibit weak and distorted prestack reflections with low coherency. Usually, the local stacking methods reveal clear reflections. However, the absolute level of amplitude spectra after such stacking experiences a substantial decline across the entire frequency band, reaching −10 to −25 dB. In addition, stacking leads to a significant and progressive loss of higher frequencies. We describe mathematical and intuitive physical models for multiplicative random noise that could consistently explain these field observations at least semiquantitatively. Multiplicative noise is represented by random timeshifts (residual statics) and random phase perturbations different for each frequency. Residual statics explain the progressive loss of higher frequencies. On the other hand, phase perturbations lead to a severe loss of coherency on prestack gathers and produce a strong downward bias or loss of broadband amplitudes after stacking. We find that both types of multiplicative noise can be physically generated by near-surface scattering layers with small-to-medium-scale geologic heterogeneities. We speculate that such multiplicative distortions can be referred to as seismic speckle noise well established in optics and ultrasonics. Furthermore, we derive the fundamental properties of how random multiplicative noise transforms while stacking. The first essential finding reveals that stacking produces an unbiased estimate of the clean signal phase. The second finding finds the mathematical relationship between the frequency-dependent loss of stacked amplitude and the standard deviation of residual statics and phase perturbations. These findings serve as a theoretical justification for the previously proposed methods of phase substitution and phase corrections and open the way to efficiently address random multiplicative noise in seismic processing.

INTRODUCTION

In exploration geophysics, it is commonly assumed that the biggest challenge of land seismic data is associated with strong near-surface arrivals (surface waves, refractions, guided modes, etc.) superimposed on top of weak but coherent reflections. It is further reasoned that, when slow near-surface arrivals are not adequately sampled (aliased), the resulting energy can appear as incoherent noise, causing ambiguity between signal and noise (Ait-Messaoud et al., 2005). In the past, large source/receiver arrays were used to suppress near-surface noise, particularly with lower apparent velocities (Meunier, 2011). However, although intraarray dense sampling was practical, 3D sampling remained more sparse for economic reasons. With time, more dense acquisition geometries (at least in two out of four spatial directions) are gradually becoming more prevalent (Regone et al., 2015), although with smaller arrays or single sensors attempting to reduce aliasing and eliminate undesirable array effects. Nevertheless, raw and processed data from desert environments often look incredibly challenging, suggesting that something else may be happening in our data. A simple illustration of this fact is that a routine first-break picking of the strongest first-arrivals events often becomes extremely challenging on single-sensor data from such regions (Khalil and Gulunay, 2011; Bakulin et al., 2019a, 2019b).

Broadly speaking, noise can be organized (coherent) or unorganized (random). If we focus on primary reflections as a seismic signal, all other coherent seismic arrivals represent organized coherent noise. Such noise can be considered deterministic. If a shot is repeated, this type of noise would perfectly reproduce. Random additive noise is another category caused by natural or manmade activities that have irregular appearances on the seismic records. If a shot is repeated, the signal remains the same but random noise changes. Because activities causing the noise occur independently

Manuscript received by the Editor 28 December 2021; revised manuscript received 23 March 2022; published ahead of production 24 May 2022; published online 20 July 2022.
[1]Saudi Aramco, EXPEC Advanced Research Center, Dhahran, Saudi Arabia. E-mail: a_bakulin@yahoo.com; ilya.silvestrov@aramco.com.
[2]Institute of Petroleum Geology and Geophysics SB RAS, Novosibirsk, Russia. E-mail: dmitn@mail.ru (corresponding author).

DOI:10.1190/geo2021-0830.1

from a seismic operation, random noise is typically not correlated with signal justifying its assumed additive nature.

A different kind of "random" noise is caused by scattering in the highly heterogeneous near-surface or deeper layers (Figure 1a). If small and medium-scale heterogeneities cause scattering, the resulting wavefield is known to change rapidly even with a slight change in an observation geometry such as source/receiver, angle, azimuth, etc. Several studies considered wavefield perturbations caused by such heterogeneities assuming that the media can be represented as a random velocity field with some stochastic properties (Ikelle et al., 1993; Shapiro et al., 1996; Sivaji et al., 2002; Borcea et al., 2006). They show that traces experience complex distortions, and the noise appears random on multichannel seismic records. Nevertheless, such noise remains perfectly reproducible, meaning that if the experiment is repeated with the same acquisition geometry, the noise will be identical because seismic scattering is a deterministic physical phenomenon.

The preceding description closely resembles what is known as speckle noise or just speckle in optics and acoustics (Goodman, 1976, 2020). In contrast to more conventional additive noise, such noise is multiplicative, meaning that the signal is subject to filtering or multiplication in the frequency domain. In optics and acoustics, speckle is generated when light interacts with rough surfaces or volumetric scatterers. In both cases, surface feature or scatterer size is smaller than the wavelength, whereas a significant number of features are present inside the Fresnel zone or the elementary scattering volume (Figure 1a, magnified). The resulting reflected light signal represents a superposition of multiple interfering arrivals with different phases. Such interference causes strong variations of amplitude/intensity that appear random and obscure optical images. Forward scattering of seismic arrivals propagating through a near surface with small-scale scatterers would lead to a very similar phenomenon manifested as random variations of amplitudes and phases of every arrival traversing through such a scattering layer. An example of a synthetic aperture radar (SAR) image with speckle noise characterized by granular amplitude/intensity distortions is shown in Figure 2a. For comparison, Figure 2b and 2c displays prestack gather and final stack images from a land single-sensor seismic data set. All images possess characteristic random granular noise that is abundantly present and does not stack out on the final image (Figure 2c). Therefore, we can refer to such distortions as "seismic speckle" — a natural extension of an established definition used in optics and acoustics.

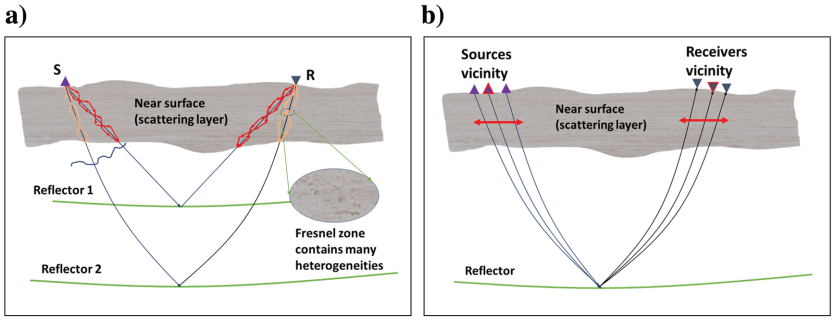

Figure 1. (a) Origin of seismic multiplicative random noise caused by seismic speckle born in the near-surface scattering layer and (b) conceptual depiction of local ensemble used for prestack data enhancement.

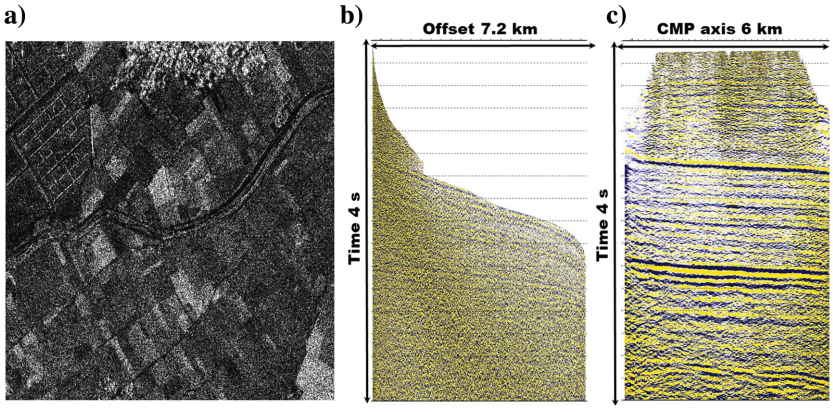

Figure 2. Images with speckle noise from SAR and seismic data: (a) SAR image from Valsesia (2020) has granular artifacts on the 2D areal image; prestack gather (b) and (c) poststack image from a land single-sensor seismic data after processing (from Bakulin et al., 2020a) show time-offset section with a "speckled" appearance due to random phase and amplitude variation. A similar granular texture of the amplitude is observed on every time slice. Neither surface objects nor subsurface geologic layers of interest under imaging are expected to contain observed high-frequency physical variation.

The multiplicative noise model itself is not new in geophysics. For example, a widely used surface-consistent deconvolution relies on a multiplicative noise model. It assumes that the frequency-dependent phase variations are caused by a combination of source/receiver coupling and near-surface effects (Taner and Koehler, 1981; Cary and Lorentz, 1993). However, multipliers in this model are presumed to be deterministic operators independent of time and satisfy the surface consistency hypothesis. Surface consistency assumes that operators depend only on source and receiver positions and offset. They are applied to the entire trace, assuming that all arrivals require identical corrections (no time dependency). Although surface-consistent deconvolution has proven useful in correcting for some phase variations in seismic data, it fails to address strong random phase variations caused by small- and medium-scale near-surface scattering. Physical scattering does not satisfy assumptions of surface consistency because interference patterns vary quickly and unpredictably in time and space. Therefore, scattering distortions are unique for each wavepath (Figure 1a) and time-dependent. In summary, geophysics thus far has only used deterministic multiplicative models with additional simplifying assumptions of surface consistency that make the problem tractable and overdetermined (the number of equations is larger than the number of unknowns). A more general multiplicative model is required to address scattering distortions. However, such a problem requires a stochastic approach (random noise) as done in speckle to become tractable.

Wave propagation theory in random media suggests that scattering noise can be represented as space- and frequency-dependent multipliers with

DOI:10.1190/geo2021-0830.1

specific distribution functions depending on the media's stochastic properties (e.g., Müller and Shapiro, 2001). However, random-media wave propagation theory developments appear far removed from seismic processing practice. Finally, seismic studies of random-media wave propagation did not relate to multiplicative speckle noise, unequivocally recognized and analyzed in acoustics and ultrasound. This study highlights the abundance and significance of a highly variable multiplicative noise in seismic data, at least in a desert environment. We believe that a stronger appreciation of multiplicative speckle noise may lead to substantial practical implications similar to what happened in optics/laser/SAR domains since the 1960s (Beckmann, 1962, 1964; Goodman, 1976, 2000, 2007, 2020; Moreira et al., 2013) and ultrasonic/acoustics fields since the 1980s (Abbot and Thurstone, 1979; Wells and Halliwell, 1981; Fink and Derode, 1998; Damerjian et al., 2014). Mitigating the multiplicative speckle noise is a complex problem that is still not fully solved (Goodman, 2020). However, the growing arsenal of methods based on powerful speckle-based statistical models led to significant advances in laser, SAR, and ultrasound imaging (Goodman, 2007; Moreira et al., 2013; Damerjian et al., 2014) as well as cross pollination between different domains (Goodman, 2020).

The optical and ultrasound domains often focus on monochromatic waves and intensity images. As a result, phase and especially the frequency dependence of the phase are less studied. In contrast, seismic data rely on broadband data where accurate reconstruction of phase information is a key to successful seismic processing and imaging. It is well acknowledged that if the amplitude spectrum is perturbed, but the phase spectrum remains intact, the main signal events can still be accurately detected in terms of the time and spatial positions (Oppenheim and Lim, 1981; Blackledget, 2006; Ulrych et al., 2007; Bakulin et al., 2020b). Although this fact is known, it often is described qualitatively, and its implications are not fully appreciated in seismic imaging. To correct this, we put a mathematical derivation in Appendix A inspired by Lichman (1999) to demonstrate that arrival time information of seismic events is encoded in the phase spectrum. More specifically, it underscores that the amplitude spectrum (equation A-3) depends only on traveltime differences. The phase spectrum is a function of actual traveltimes (equation A-4). This critical fact is a cornerstone for understanding the effects of multiplicative noise and designing methods to mitigate it.

Bakulin et al. (2018a, 2020a) show that reflections can be extremely weak and distorted in land seismic data when acquired with small arrays or single sensors. Weak signals must be collected and averaged using the multichannel seismic data redundancy to become processable and imageable. Furthermore, phase variations appear to be a critical culprit behind severe distortions. Enhancement techniques use information about local traveltimes of desired arrivals to provide output data with an improved signal-to-noise ratio (S/N). Bakulin et al. (2020b, 2020c, 2021) put forward phase substitution and phase correction methods. They speculate that the phase spectra of enhanced data should be a relatively close estimate of the local phases of "actual" undistorted signals. In other words, they assume that the positions and phases of reflected events in a trace become more or less correct after enhancement. Khalil and Gulunay (2011) also make a similar assumption for the first arrivals when deriving intraarray statics for single-sensor data from the desert environment. This study puts forward a physical and mathematical model that can theoretically justify this statement using realistic assumptions about random multiplicative noise.

We start the paper by examining typical seismic records from the desert environment exhibiting the effects of complex surface scattering and summarizing the main observations on how such data transform during the local stacking process. Next, we show the numerical modeling results with a near-surface clutter layer that replicates essential features of the real data. Modeling confirms that multiple scattering causes strong frequency-dependent phase distortions that appear random and cause severe loss of coherency. We then build a mathematical model for seismic speckle approximating the noise as random multiplicative noise. Finally, we examine the effects of random multiplicative noise on local stacking. Two remarkable fundamental properties are discovered. First, summation leads to an estimate of the true undistorted phase spectrum. Second, the amplitude of the stacked response shows a characteristic frequency-dependent loss that closely replicates observations from the field data. These findings cement our understanding of the seismic speckle as a random multiplicative noise abundantly present in challenging seismic data. At the same time, discovered fundamental properties pave the way to the elimination of seismic speckle by novel processing algorithms. This new recognition also opens the door to transfer learning from a plethora of existing approaches to suppress multiplicative speckle noise developed in optics, acoustics, and ultrasonic.

WHAT DO WE OBSERVE IN REAL DATA?

We first examine two different data sets from the desert environment paying attention to subtle details such as the variation of phase and amplitudes and their transformation during the stacking process. A common-midpoint (CMP) gather from the first 3D data set is shown in Figure 3. This is the legacy data with 72-geophone groups from a very challenging geophysical area. Although ordinarily, such legacy data are of a high S/N, this case represents an exception from an area with the most complex near surface. The input data have already been passed through a standard time processing flow for land data, including linear and random noise removal, surface-consistent scaling, deconvolution, etc. (see e.g., Taner and Koehler, 1981; Cary and Lorentz, 1993; Chan and Stewart, 1994; Meunier, 1999; Liu et al., 2006). Nevertheless, the prestack signal remains very weak, and there are no visible reflections in the gather. In addition, we observe that the entire gather shown in Figure 3a remains similarly speckled from top to bottom and from small offset to large. Although it is not uncommon that unsuppressed remnants of intense direct and scattered groundroll often can create a residual "noise cone" restricted by direct surface-wave arrivals, even events outside such a noise cone remain obscured in this case, suggesting a different mechanism for distortions. Figure 3b shows the same CMP gather after data enhancement based on local stacking using nonlinear beamforming (NLBF) (Bakulin et al., 2020a). The detail of the actual enhancement technique itself is of secondary importance here. Other local-stacking techniques could achieve a similar result (Baykulov and Gajewski, 2009; Berkovitch et al., 2011; Buzlukov and Landa, 2013; Bakulin et al., 2018a, 2018b). We note that approximately 200 neighboring traces are used in the local summation to enhance each original trace in this case. After the enhancement, the reflections are easily recognizable in the entire offset range. However, the high-frequency content of the signal becomes strongly suppressed (Figure 3c) whereas reflection events become overly smoothed. In other words, beamforming replaces the jittery amplitude and phase along the event with relatively smoothly varying quantities.

We jump to a second data set from a more recent and dense acquisition using smaller nine-geophone arrays in a different area also from the desert environment. Again, we observe very similar behavior. Figure 4a shows a CMP gather after processing with a little visible signal. Local stacking with NLBF reveals underlying reflections (Figure 4b). Likewise, higher frequencies greater than 20 Hz are greatly diminished (Figure 4c).

In addition to challenging reflection data quality, such data also typically exhibit very complex first arrivals. Khalil and Gulunay (2011) and Bakulin et al. (2018b, 2019b) present multiple examples of jumbled early arrivals with low coherency from nine-geophone arrays and single-sensor data. To enable first-break picking and full-waveform inversion (FWI), early arrivals must be significantly preprocessed using local stacking. Finally, there were cases of single-sensor data deemed not usable for near-surface model building using traveltime tomography and FWI. Suppose we distill common traits shared by these and many other challenging data sets from the desert environment. In that case, we arrive at three critical observations:

Observation 1: Even after sophisticated processing, reflections on prestack data remain distorted with low coherency or even untrackable. Such distortions are not localized in time-space but instead spread over the entire gather. In addition, first arrivals also are cluttered, making it difficult to pick first breaks or use early arrivals for FWI.

Observation 2: After applying local stacking, reflections crop up very clearly, but the absolute level of amplitude spectra experiences significant bias downward (−15 to −20 dB in the shown example) across all frequencies.

Observation 3: There is a significant and progressive loss of higher frequencies after local stacking.

Although it is expected that stacking in the presence of residual statics acts as a low-pass filter (Berni and Roever, 1989; Marsden, 1993), the lowest frequencies below 10–20 Hz should not be significantly affected. However, we observe −15 to −20 dB amplitude bias at those same low frequencies, even though a standard fold normalization is used in stacking. Although seismic waves do attenuate with depth, note that we operate with prestack events already propagated to the same depth in local stacking. We merely examine the transformation of the frequency content of the same event before and after stacking. Therefore, the loss of higher frequencies at hand (observation 3) has little to do with any actual attenuation during propagation. Finally, we stress that data are examined after preprocessing that include conventional linear and random noise attenuation steps in both examples. Something does not add up in a traditional point of view of coherent reflections superimposed by "background near-surface noise," even if we allow some residual statics to be present. We shall seek and offer an alternative explanation to explain observations 1–3 without contradictions. This alternative explanation is a distortion of the signal itself caused by medium- and small-scale scattering (Figure 1a).

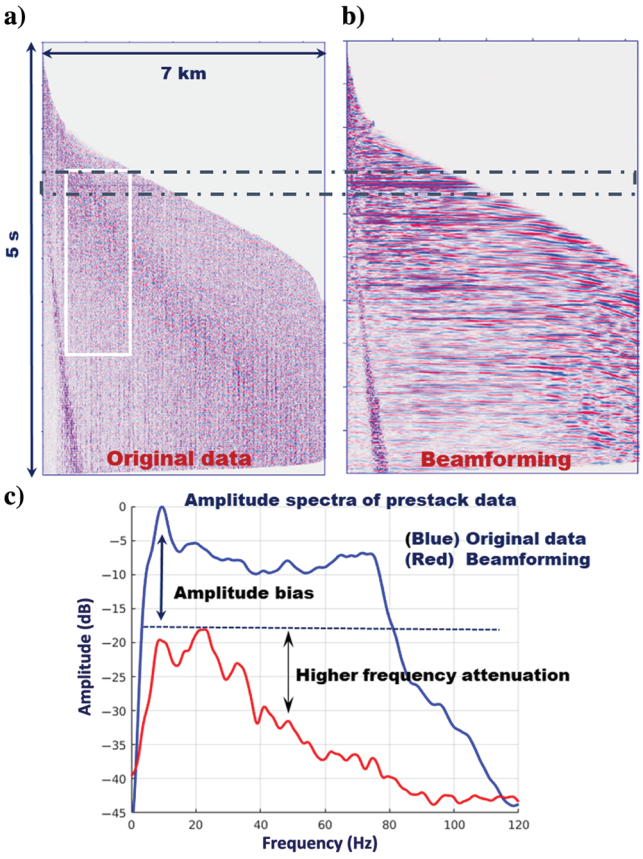

Figure 3. NMO-corrected CMP gather from an area with complex near surface: (a) after standard processing, (b) the same gather, but after additional enhancement with NLBF based on local stacking (aperture of 300 m), and (c) amplitude spectra of original (blue) and enhanced (red) data. Observe low coherency in (a) and high coherency in (b), but associated with significant amplitude bias and progressive loss of higher frequencies.

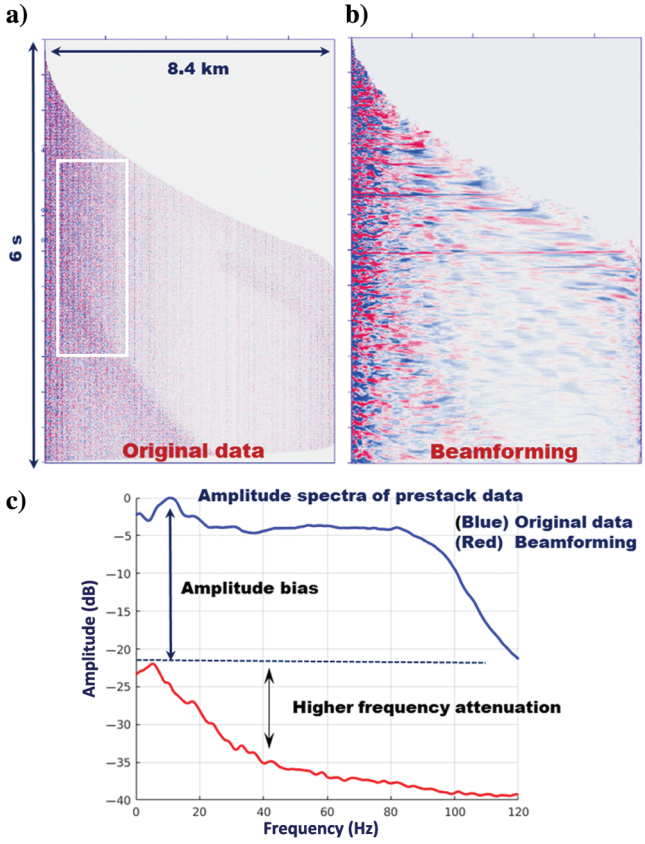

Figure 4. Same as Figure 3, but for a different data set from the desert environment. The beamforming aperture is 300 m.

DOI:10.1190/geo2021-0830.1

NEAR-SURFACE SCATTERING LAYER AND ITS IMPACT ON SIGNAL PHASE

To illustrate the impact of scattering on the seismic signal, we resort to the simple acoustic model shown in Figure 5a with a near-surface scattering layer. We deliberately select acoustic modeling to exclude the effects of groundroll, converted waves, and other elastic arrivals. Thus, we take a large part of the organized coherent near-surface noise out of the equation from the start to emphasize that the proposed mechanism for signal distortion does not require elastic noise. Instead, only sufficient small- and medium-scale heterogeneities in the near-surface layer are necessary to create volumetric random scattering noise referred to as speckle in optics and ultrasonics.

To interpret somewhat jumbled seismic gathers, let us remind ourselves of the meaning of coherency that we usually expect on multichannel seismic records in terms of the signal phase. A visible coherent event in multichannel data corresponds to a time window with mild phase angles variations. A constant phase surface provides a coherent event in multichannel data in a noise-free case. Let us illustrate this statement using synthetic and real data.

We contrast two common-shot gathers calculated using the finite-difference modeling with the same subsurface model except for the differing near-surface layer. The first case has a homogeneous near-surface layer (Figure 5b). In contrast, the second has a near-surface scattering layer (Figure 5c) modeled as a random clutter.

For analysis, we choose the third reflection event marked by the arrows. A time window with a width of 200 ms was extracted along the chosen reflector. Corresponding windowed data are shown in Figure 6 after normal moveout corrections. As one can see, the target reflected arrivals are perfectly aligned for "clean" data (homogeneous near surface). In contrast, the same arrival is severely broken up in the presence of a near-surface scattering layer (Figure 6b). A Fourier transform is applied to the extracted windowed data. In Figure 7, we present phase angles as a function of trace index at a fixed frequency of 10 and 20 Hz (dominant frequency used in acoustic finite-difference modeling). Phases of clean data are nearly constant, whereas phases of perturbed data vary abruptly. A similar behavior holds for any other frequency with randomly looking phase jumps. In addition, there is no apparent connection between phase jumps observed at different frequencies. Such random phase fluctuations are the primary cause of why one cannot see coherent arrivals in the "perturbed" data (Figure 6b). After beamforming, phase angles acquire a relatively smooth behavior (Figure 7). As a result, one can see the coherent event in the corresponding gather (Figure 6c).

From this numerical experiment, we can say that the main reason why even after elaborate processing, one can barely see coherent events in land seismic data is random phase variations of "distorted reflections." We do call them distorted reflections for two main reasons. First, they reside in the same time window as undistorted arrival in the clean model, called ballistic arrival. Second, they are not contaminated by the superposition of "background" noise but rather consistently experience complex interference. Random-like phase variations make reflections poorly visible. Displaying amplitude at a fixed frequency (Figure 8), we observe random-like fluctuations, characteristic for optical or ultrasound speckle noise (Goodman, 2007). Local stacking of data with such phase perturbations leads to comparable amplitude bias and progressive loss of higher frequencies, as noted in the field data (observations 2 and 3).

Similar phase behavior is seen in real seismic data. Figure 9 presents the time-windowed data taken from NMO-corrected CMP gather shown in Figure 3a. For analysis, we time-gated a single visible reflected event. Phase angles taken at the frequencies 10 and 30 Hz for the original and enhanced data are presented in Figure 10. The phase angles of the original data vary chaotically in the allowable interval $[-\pi, \pi]$. In contrast, phases of enhanced data have very smooth variations.

In the synthetic example with the acoustic model, observed noise allows a more straightforward physical interpretation. We have eliminated surface waves and shear waves from the equation. Therefore, we are left with a scattering of the P-wave energy only. It may be tempting to assume that what we see in Figure 5c is a superposition of many diffractions from the near-surface scatterers that overlay and complicate undistorted primary reflections. However, simple numerical experiments disprove such an interpretation.

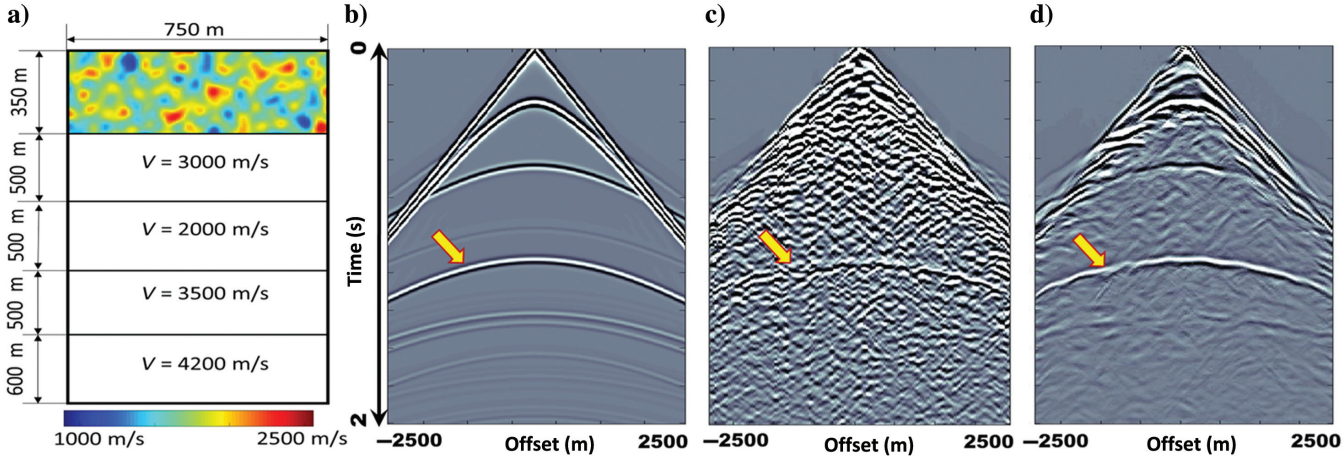

Figure 5. The synthetic model with near-surface clutter and associated data: (a) five-layer acoustic model with near-surface layer modeled as a random clutter (velocity variation of 200 m/s and correlation length of 30 m), (b) common-shot gather when a homogeneous layer replaces near-surface clutter, (c) gather in the model (a) with near-surface clutter, and (d) enhanced gather from (c) after NLBF. The arrow marks the target reflector. Ricker wavelet with 20 Hz central frequency is used as a source signature.

DOI:10.1190/geo2021-0830.1

Figure 11a–11c shows wavefields in the full five-layer model versus reduced two-layer model (no deep reflectors) and their difference. Figure 11b shows the entire scattered wavefield induced by heterogeneities of the near-surface layer. As expected, such noise is the strongest near early arrivals (single scattering). It decays away from the first breaks or toward later times, as is expected for multiple scattering. In particular, Figure 11c shows the difference containing four primary reflectors and all noise generated squarely by themselves. First, we can see that reflection events on the full gather (Figure 11a) and difference field (Figure 11c) remain similarly damaged, suggesting that the superimposed background noise removed by differencing is not a significant explanation to observed distortions. In addition, the reflected events themselves induce the halos around them. Finally, stronger reflectors create more intense halos (compare Figures 5b and 11c).

Figure 11d further emphasizes the point that a single direct arrival propagating through the near-surface layer is indeed strongly distorted in the vicinity of the ballistic arrival itself. All these observations could be readily explained by the mechanism from Figure 1a, typical for (volumetric) speckle noise. Comparing reflector R3 in Figure 11c with direct arrival in Figure 11d, it is evident that distortions due to two-way propagation are more pronounced than those caused by a one-way transmission through a near-surface scattering layer. Because reflections and multiples themselves induce scattering noise, it is plausible to relate Figures 3a, 4a, and 11a. In the synthetic case, only a handful of reflectors induced overlapping halos of scattering noise. The desert environment is characterized by an almost continuous sequence of subsurface reflectors with strong contrasts (Alexandrov et al., 2015). Therefore, the proposed mechanism can plausibly explain the almost continuous carpet of scattering noise on real data, supporting the previous observation 1.

We conclude that the noise mechanism is likely related to the speckle concept, as depicted in Figure 1a. Many forward-scattered waves arrive near-ballistic traveltime, creating a complex interference that jumbles the total waveform (Figure 11c and 11d). Prunty and Snieder (2017) highlight the critical role of such near-ballistic forward scattering to explain the memory effect associated with acoustic speckle. The multiplicative nature of speckle noise explains why a stronger signal generates stronger noise. The sequence of primary reflections and multiples seen in Figure 11a induces corresponding "halos" or "ornaments" around each of them, with stronger events creating more energetic halos. Seismic processing and imaging rely on tracking and eventually summing redundant seismic traces providing illumination from multitudinal offsets and azimuth. In particular, time processing and imaging rely on consistent waveforms within prestack data that imply smoothly varying phases. We observe that local stacking performs phase "ordering." As a result, events become coherent and visible (Figures 6c and 7), thus conditioning the data for processing and imaging. However, significant side effects occur while stacking, such as amplitude bias and loss of higher frequencies that limit the vertical resolution of the seismic images. Currently used seismic processing algorithms are not designed to tackle random multiplicative noise. If we know the true velocity model, migration may correct such phase variations and lead to correct images. However, it is almost impossible to precisely recover small-scale velocity variations in practice. If we only estimate the smoothed background velocity model, migration would similarly suffer from phase perturbations, producing poor focusing (He et al., 2017). Armed with the preceding intuitive understanding of the nature of seismic speckle (Figure 1a) and numerical experiments, we can mathematically describe it as multiplicative random noise. As outlined in the "Introduction" section, such a description is well established in optics and ultrasound. In the next section, we put forward a mathematical model of multiplicative random seismic noise and analyze how it affects the amplitude and phase of the data during the local stacking process.

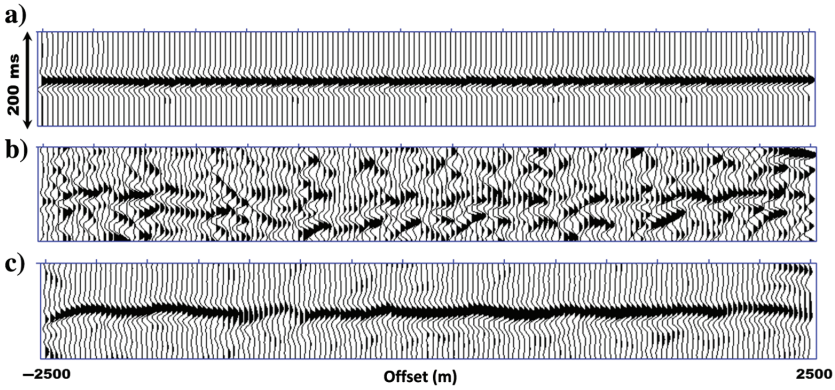

Figure 6. Time-windowed (200 ms) synthetic data around the target reflector from Figure 5: (a) clean data with the homogeneous near surface, (b) perturbed data with near-surface scattering layer, and (c) data from (b) enhanced using beamforming.

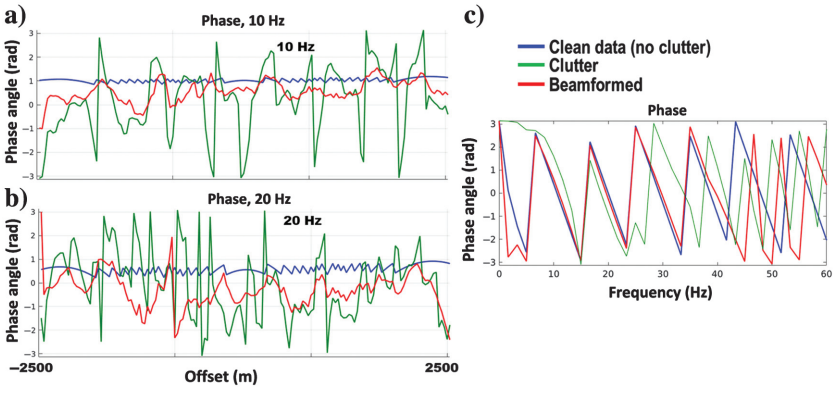

Figure 7. Signatures of the phase spectrum for data from Figure 6: (a) phase extracted at a fixed frequency as a function of trace index at 10 Hz, (b) same as (a) but for 20 Hz, and (c) phase spectrum of a single trace at an offset of 500 m. The blue lines denote clean data, green marks "clutter" data, whereas red corresponds to enhanced data after beamforming. Observe substantial phase variations of data with the clutter (green). In contrast, beamformed data (red) have a smoothly varying phase closer to the clean phase (blue). Note that the phase of the beamformed data approaches the clean signal phase below 40 Hz (c).

MATHEMATICAL MODEL OF SEISMIC TRACE WITH MULTIPLICATIVE RANDOM NOISE AND ITS TRANSFORMATION WHILE STACKING

Random model of speckle and interpretation of ensembles in local stacking

In the typical speckle treatment (Goodman, 1976, 2000), it is reasoned that we lack an exact knowledge of the detailed microscopic structure that causes multiple forward scattering shown in Figure 1a. Therefore, it is necessary to discuss the properties of speckle patterns in statistical terms. The statistics of interest are defined over an ensemble of different experiments. If we fix the source-receiver pair, a different experiment will correspond to placing another fine-scale realization of near-surface heterogeneity (with the same statistical properties), generating another version of the distorted or noisy outcome. For a fixed pair, such changes need to be made only in the vicinity of the wavepath because properties outside those areas would not affect the outcome. Because the outcome of the interference changes quickly (Goodman, 2000, 2020; Fink and Derode, 1998), another way to produce a different experiment is to change the source and/or receivers' positions slightly. The wavepath in the near-surface layer would shift, leading to another interference outcome. Let us restrict our initial investigation to the local stacking of prestack data instead of global stacking. Although generating stacked or migrated images may involve huge ensembles such as CMP gathers with wavepaths traversing vast amounts of the subsurface, this is not the case for local data enhancement that only stacks a limited amount of data inside a local ensemble (Buzlukov and Landa, 2013; Bakulin et al., 2018a, 2020a). By design, a typical ensemble of traces is drawn from a certain spatial vicinity limited by a local aperture (Figure 1b). Bakulin et al. (2020a) discuss ensemble selection and typical examples of various ensembles represented by local subsets of various gathers such as CMP, cross spread, etc. Therefore, all traces inside such an ensemble share two key commonalities.

1) All traces are expected to contain similar reflected signals produced by a limited segment of a geologic interface of interest. Hence, we assume that, in the absence of multiplicative noise, the reflected signals detected by each trace are nearly identical inside the ensemble (after local moveout correction).
2) Each trace carries a different realization of multiplicative noise. By design with sources and receivers selected within a limited vicinity, all wavepaths are similarly clustered around a certain vicinity of the near-surface scattering layer (Figure 1b). As a result, exact microscopic properties (e.g., the positions of small scatterers) inside each wavepath differ and lead to different interference patterns on each trace. However, assuming that statistical properties (e.g., the number of scatterers per unit cell and their contrast) are fixed or slowly varying between neighboring wavepaths — we can consider traces from the ensemble providing distinct realizations of the same seismic speckle.

One point to mention here is that reflections from different depths would lead to a different scattering distortion because their wavepaths in the highly scattering near surface could be sufficiently different (Figure 1a), even though both events belong to the same seismic trace. Let us suppose that near-surface properties vary laterally and with depth. In that case, distinctive distortions are expected for different reflectors, suggesting that simplified assumptions such as surface consistency do not hold for the case of complex 3D wave propagation when small-scale heterogeneities are present in the near surface.

Multiplicative random noise model

Because the signal itself induces speckle noise, it is universally accepted from optics to ultrasound that it may be accurately represented as random multiplicative noise (Goodman, 1976, 2020; Jain, 1989; Moreira et al., 2013; Damerijan et al., 2014). Based on the considerations previously, we represent the trace recorded by the kth channel of the ensemble as

$$x_k(t) = r_k(t) * s(t) + n_k(t), \tag{1}$$

where $s(t)$ is the desired signal, $r_k(t)$ is random multiplicative noise with the same distribution within all channels, $n_k(t)$ is additive random noise, "*" denotes convolution, and $k = 1, \ldots, K$ (K is the number of the channels in the local ensemble).

In the Fourier domain (equation 1), it can be written as

$$X_k(\omega) = R_k(\omega)S(\omega) + N_k(\omega), \tag{2}$$

where X_k, R_k, S, and N_k are Fourier transforms of the corresponding time-domain functions in equation 1.

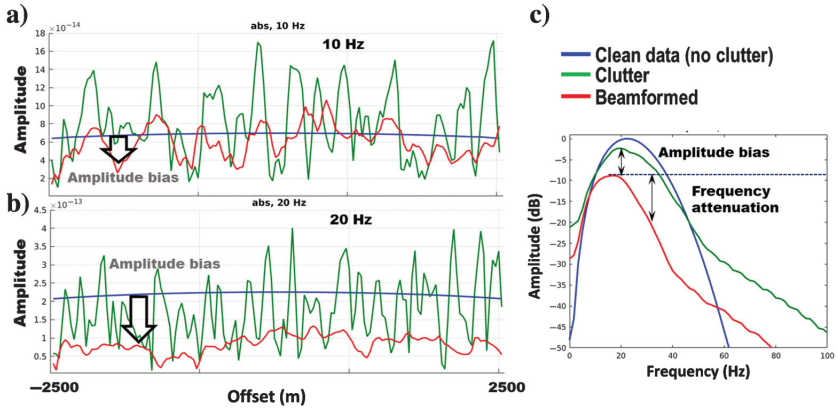

Figure 8. Signatures of the amplitude spectrum for data from Figure 6: (a) amplitude extracted at a fixed frequency as a function of trace index at 10 Hz, (b) same as (a) but for 20 Hz, and (c) averaged amplitude spectra of all traces inside the window. The blue lines denote clean data, green marks perturbed data, whereas red corresponds to enhanced data after beamforming. Observe random variation of the data with near-surface scattering layer (green) around a certain trend. In addition, pay attention to the amplitude bias marked by arrows with the average amplitude of beamformed data (red) being lower than distorted data before stacking (green). Finally, spectrum (c) exhibits characteristic amplitude reduction and roll-off at high frequencies, similar to what is seen in real data from Figures 3c and 4c.

It is assumed that additive noise $N_k(\omega)$ is uncorrelated between different channels and has a zero mean, i.e., $E[N_k(\omega)] = 0$, where an E stands for the mathematical expectation. In addition, signal and noise are assumed to be uncorrelated.

Local stacking as an approximation of mathematical expectation of random trace

The effect of stacking on additive random noise is well understood. Hence, it serves as a cornerstone of increasing S/N during acquisition, processing, and imaging (Meunier, 2011). However, since multiplicative noise is not well recognized in seismic data, a similar understanding needs to be built for seismic multiplicative noise because stacking is the essential element of processing and imaging. Therefore, we shall establish some basic foundation using the simplified mathematical model (equation 1).

The local stack over an ensemble of traces is calculated as

$$\bar{X}(\omega) = \frac{1}{K}\sum_{k=1}^{K} X_k(\omega). \tag{3}$$

A large ensemble of several hundreds of traces for local stacking provides a sufficient data set to approximate the mathematical expectation of the described random process. Let us examine its information content and properties. Mathematically, this is expressed as

$$\begin{aligned}\bar{X}(\omega) \;&\approx E[X_k(\omega)] = E[R_k(\omega)S(\omega)] + E[N_k(\omega)] \\ &= S(\omega)\; E[R_k(\omega)].\end{aligned} \tag{4}$$

Here, we assume that the signal remains constant and assume that the additive noise's mathematical expectation vanishes. Equation 4 provides the theoretical prediction of how summation transforms the amplitude and phase of the stacked result. Most importantly, it allows abstracting from specific fine-scale geologic heterogeneity and replaces it with just knowledge of statistical distribution. Because we assume fixed flat signals, then the function

$$\Phi(\omega) = E[R_k(\omega)] \tag{5}$$

can be thought of as a distorting filter $\Phi(\omega)$ applied to the original signal as shown in equation 4.

Let us now consider two types of multiplicative noise. The first type is inspired by numerical experiments and data observations shown in Figures 5–11, summarized as random frequency-dependent phase fluctuations. The second is the well-known residual statics or random timeshifts between channels. Initially, we analyze the effects of each type of multiplicative noise on stacking separately. Finally, we consider the combined effects of both types of noises on stacked amplitude and phase and relate the results to real data observations.

The first type of multiplicative random noise: Random frequency-dependent phase fluctuations

Let us consider multiplicative seismic speckle noise as random frequency-dependent phase fluctuations acting on each time window:

$$R_k(\omega) = e^{i\varphi_k(\omega)}. \tag{6}$$

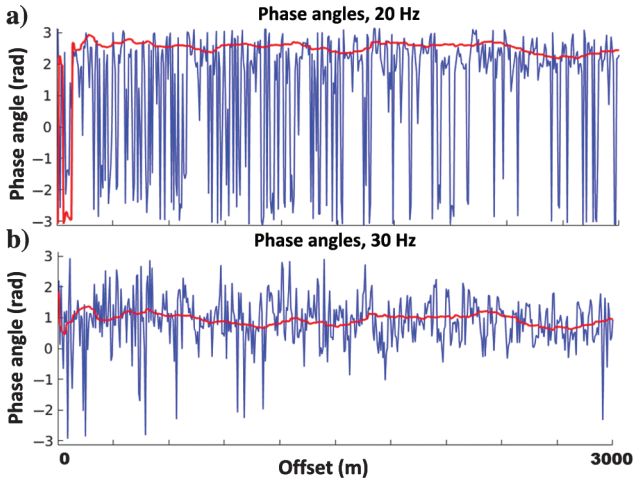

Figure 10. Phase angles for land data from Figure 9: (a) phase angles (in radian) at 20 Hz as a function of trace index and (b) phase angles at 30 Hz as a function of trace index. Observe large random phase variations of original data (blue) with a much smoother phase of beamformed data (red). Notice no apparent correlation between phase perturbations at (a) 20 Hz and (b) 30 Hz.

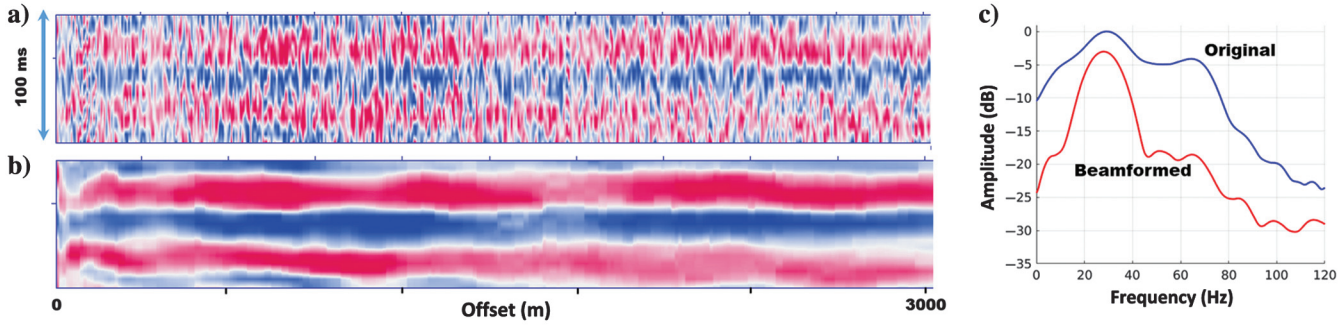

Figure 9. Time-windowed land data around the target reflector (100 ms) taken from Figure 3a (blue window): (a) original data, (b) data after beamforming based on local stacking, and (c) associated absolute (nonnormalized) amplitude spectra.

DOI:10.1190/geo2021-0830.1

Following the footsteps of an established model of speckle noise as a random-walk phenomenon (Goodman, 1976, 2000, 2020), we assume that, at a given frequency ω, random variables $x = \varphi_k(\omega)$ are independent for all channels and have the same probability density function $P(\omega; x)$ at a given frequency ω.

Some general properties of stacked sums with multiplicative noise can be established by defining the distributions' symmetry. For example, using a known formula for the mathematical expectation of a random variable function, we can write (equation 5) as

$$\Phi(\omega) = \int_{-\infty}^{\infty} P(\omega; x) e^{ix} dx. \tag{7}$$

Equation 7 leads to an important property that if the probability density function of the phase fluctuations of the multiplicative noise is even, i.e., $P(\omega; x) = P(\omega; -x)$ (implying that the expected value is zero), then $\Phi(\omega)$ is real-valued, and equation 4 transforms to

$$E[X_k(\omega)] = |S(\omega)| e^{i\varphi_S(\omega)} \Phi(\omega), \tag{8}$$

where $|S(\omega)|$ is the amplitude spectrum of the signal and φ_S is its phase. We can make essential conclusions under these rather general assumptions without specifying the actual symmetric distributions of the phase perturbations. First, we observe the phase "cleanup" process in which random symmetric phase perturbations average out during stacking and lead either to signal phase (if $\Phi(\omega) > 0$), or flipped signal phase rotated by π (if $\Phi(\omega) < 0$). Second, real-valued $\Phi(\omega)$ describes the transformation or filtering of the signal amplitude spectra during stacking. To arrive at quantitative numerical results, let us derive a specific form of $\Phi(\omega)$ for the case of normal and uniform distribution of phase perturbations.

Normal (Gaussian) distribution of phase fluctuations

If random variables $x = \varphi_k(\omega)$ describing phase perturbations all have the same normal (Gaussian) distribution with zero mean and standard deviation $\sigma_\varphi(\omega)$, then

$$P(\omega; x) = \frac{1}{\sqrt{2\pi}\sigma_\varphi(\omega)} e^{-\frac{x^2}{2\sigma_\varphi^2(\omega)}}. \tag{9}$$

After substitution of expression 9 in expression 7, it follows that

$$\Phi(\omega) = e^{-\frac{\sigma_\varphi^2(\omega)}{2}}. \tag{9a}$$

As a result, mathematical expectation can be expressed as

$$E[X_k(\omega)] = |S(\omega)| e^{i\varphi_S(\omega)} e^{-\frac{\sigma_\varphi^2(\omega)}{2}}. \tag{9b}$$

Although it was predicted from symmetry considerations, it is nevertheless remarkable to note that the resulting phase spectrum after stacking in expression 9b is the same as the phase of the clean signal, i.e.,

$$\arg\{E[X_k(\omega)]\} = \varphi_S(\omega), \tag{10}$$

whereas a real-valued filter reduces amplitude compared with a clean signal. If standard deviations remain constant for all frequencies, amplitude loss is identical across the entire band. If we assume that the standard deviation increases with frequency (i.e., larger phase perturbations at higher frequencies), then the loss of signal amplitude after stacking would progressively increase with frequency.

Symmetric uniform distribution of phase fluctuations

If we assume that those phase perturbations $\varphi_k(\omega)$ are uniformly distributed within the interval $[-\varphi_0(\omega), \varphi_0(\omega)]$ (in radians), then probability density function has the form:

$$P(\omega; x) = \begin{cases} \frac{1}{2\varphi_0(\omega)}, & \text{if } |x| < \varphi_0(\omega) \\ 0, & \text{if } |x| > \varphi_0(\omega) \end{cases}, \tag{11}$$

$$\Phi(\omega) = \frac{\sin[\varphi_0(\omega)]}{\varphi_0(\omega)}, \tag{11a}$$

with mathematical expectation

$$E[X_k(\omega)] = |S(\omega)| e^{i\varphi_S(\omega)} \frac{\sin \varphi_0(\omega)}{\varphi_0(\omega)}. \tag{11b}$$

Again, it is remarkable to note that, after taking the mathematical expectation, phase distortions are eliminated, and the resulting phase spectrum of the broadband signal after stacking tracks the phase of the clean signal provided $\varphi_0 < \pi$. Note that if $\varphi_0(\omega) = \pi$, then $E[X_k(\omega)] = 0$ that could be interpreted as perfect destructive interference. Finally, if $\varphi_0 > \pi$, then the stacked phase still tracks the clean signal phase but with the opposite sign (polarity flip). As in the previous example, the stacked amplitude is reduced compared with the clean signal, although the real-valued factor has a more complex frequency dependency.

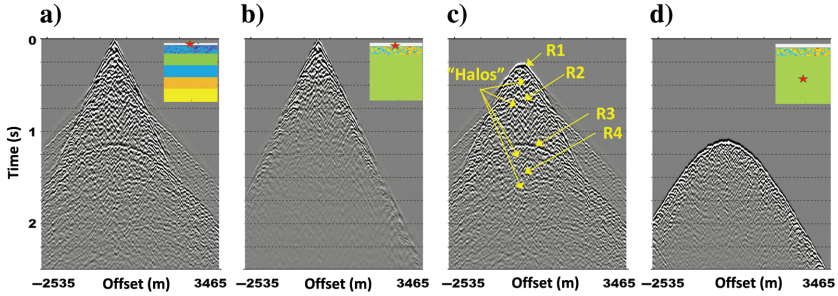

Figure 11. Visualizing multiplicative scattering noise: (a) surface shot gather in five-layer model with near-surface scattering layer from Figure 5a, (b) same shot in the presence of near-surface clutter layer, but with deep reflections eliminated (layers replaced by homogeneous half-space), (c) difference between (a and b) highlighting distorted reflection events with signal-induced halos, and (d) buried shot in the same model as (b) showing the impact of near-surface scattering layer on one-way propagation. Reflector R3 in (c) with two-way propagation appears more broken when compared with direct arrival in (d) experiencing single transmission through near-surface scattering layer.

The second type of multiplicative noise: Random timeshifts between channels (residual statics)

Although residual statics is a well-known type of seismic distortion, it also can be mathematically described as a specialized type of multiplicative noise caused by random time shifts τ_k between channels. In this case, multiplicative noise has a specific form:

$$R_k(\omega) = e^{-i\omega\tau_k} \tag{12}$$

and

$$\Phi(\omega) = E[e^{-i\omega\tau_k}]. \tag{13}$$

Please note that while it may appear as if the residual statics may be represented as a particular case of the first type of multiplicative noise, this is generally not the case. Indeed, once a specific value of static shift is drawn for a selected channel, then phase perturbations versus frequency for multiplicative noise (equation 12) would always follow a linear dependence. Therefore, phase perturbations are synchronized. In contrast, the first type of multiplicative noise is entirely random fluctuations occurring within a single trace at each frequency. In other words, if phase perturbations are visualized for each trace realization, then the first type would exhibit random jumps in phase with frequency (as in Figure 10). In contrast, phase variations for the second type would follow a straight line as a function of frequency.

Normal (Gaussian) distribution of timeshifts (residual statics)

Let the residual statics τ_k have a normal distribution with zero mean and the same standard deviation σ_τ:

$$P(x) = \frac{1}{\sqrt{2\pi}\sigma_\tau} e^{-\frac{x^2}{2\sigma_\tau^2}}. \tag{14}$$

Then, associated quantities can be expressed as

$$\Phi(\omega) = e^{-\frac{\omega^2\sigma_\tau^2}{2}}, \tag{14a}$$

$$E[X_k(\omega)] = |S(\omega)|e^{i\varphi_s(\omega)}e^{-\frac{\omega^2\sigma_\tau^2}{2}}. \tag{14b}$$

We arrive at the same conclusion that the phase spectrum of the stack (equation 14b) is the same as that of the clean signal, i.e., expression 10 is valid again. Amplitude experiences exponential loss with frequency. For field arrays, so-called intraarray residual statics were always blamed as a significant analog grouping limitation that reduces high-frequency content. Exponential decay was noted by Berni and Roever (1989) in an alternative derivation that did not use a multiplicative noise model and did not analyze the phase behavior.

Symmetric uniform distribution of timeshifts (residual statics)

Let residual statics τ_k now be uniformly distributed within the interval $[-\tau_0, \tau_0]$. Then, probability density function has the form:

$$P(x) = \begin{cases} \frac{1}{2\tau_0}, & \text{if } |x| < \tau_0 \\ 0, & \text{if } |x| > \tau_0 \end{cases}, \tag{15}$$

$$\Phi(\omega) = \frac{\sin(\omega\tau_0)}{\omega\tau_0}, \tag{15a}$$

$$E[X(\omega)] = |S(\omega)|e^{i\varphi_s(\omega)}\frac{\sin(\omega\tau_0)}{\omega\tau_0}. \tag{15b}$$

The mathematical expectation has a similar structure with the phase spectrum of the signal multiplied by the real-valued amplitude loss factor that could change the sign with frequency. We further observe that the amplitude loss factor $\sin(\omega\tau_0)/\omega\tau_0$ oscillates and has periodic notches at $\omega\tau_0 = \pi, 2\pi, 3\pi, \ldots$, where the change of sign occurs. Before the first notch $\omega = \pi/\tau_0$, the stacked phase would be equal to the signal phase, whereas it will become rotated by π after that. A similar pattern repeats for subsequent notches.

For small residual statics, the first notch also may happen at a frequency exceeding the maximum frequency $f_{\max}$ of the broadband signal. In this case, the stacked trace will equal the clean signal. Such a case occurs when the following condition is satisfied

$$f_{\max} < \frac{1}{2\tau_0}. \tag{16}$$

The joint effect of residual statics and frequency-dependent random phase fluctuations

Let us consider the last case when both types of multiplicative noise (equations 6 and 12) are present. Assuming that τ_k and $\varphi_k(\omega)$ are independent of each other, we obtain

$$\Phi(\omega) = \iint_{-\infty}^{\infty} P^{(1)}(x)P^{(2)}(y)e^{-i(\omega x+y)}dxdy, \tag{17}$$

where $P^{(1)}$ and $P^{(2)}$ are the probability density functions of variables τ_k and φ_k, respectively.

If phase fluctuations and random timeshifts are normally distributed with standard deviations σ_φ and σ_τ, respectively, then the mathematical expectation is given by

$$E[X_k(\omega)] = |S(\omega)|e^{i\varphi_s(\omega)}e^{-\frac{\omega^2\sigma_\tau^2}{2}}e^{-\frac{\sigma_\varphi^2}{2}}. \tag{18}$$

Likewise, if phase perturbations and random timeshifts are uniformly distributed with intervals $[-\varphi_0(\omega), \varphi_0(\omega)]$ and $[-\tau_0, \tau_0]$, respectively, we arrive at the following mathematical expectation:

$$E[X_k(\omega)] = |S(\omega)|e^{i\varphi_s(\omega)}\frac{\sin(\omega\tau_0)}{\omega\tau_0}\frac{\sin(\varphi_0(\omega))}{\varphi_0(\omega)}. \tag{19}$$

Similar conclusions apply to both cases. For the normal distribution, the phase of mathematical expectation is equal to the clean signal phase, whereas the amplitude loss factor is a product of two terms — one caused by phase perturbations and another by residual statics.

SYNTHETIC SIMULATIONS OF LOCAL STACKING WITH MULTIPLICATIVE RANDOM NOISE

For numerical simulations, let us consider a simple case when the signal is fixed and represented by the Klauder wavelet (Figure 12), typical of land vibroseis acquisition after correlation. First, an ensem-

DOI:10.1190/geo2021-0830.1

ble of traces is generated using different realizations of multiplicative noise (Figure 13) following a mathematical model (equation 1). Then, we numerically stack traces from the ensemble (with a finite and realistic number of traces) and compare with the amplitude and phase predicted by theoretical equations for the preceding mathematical expectation. Our goal is to validate the usefulness of the theoretical predictions for realistic local stacking scenarios with a limited number of traces.

Example 1. Random timeshifts between channels (stack of 1000 traces)

We first perform a numerical simulation of the effect of residual statics on stacked amplitude and phase and compare them with the theoretical formulas. We consider normal and uniform distributions to seek an initial indication of which type may provide a better match to the preceding experimental observations. We use an ensemble of 1000 traces that could be a typical number for local stacking enhancement of high-density 3D seismic land data with medium and large apertures of 200–400 m (Bakulin et al., 2020a).

Normal distribution of residual statics

We start with the normal distribution of residual statics and consider two realistic cases of $\sigma_\tau = 4$ ms and $\sigma_\tau = 8$ ms. Figure 14 visualizes the distribution of residual statics for one ensemble in the case of $\sigma_\tau = 8$ ms. Although approximately 2/3 of the channels have statics less than the standard deviation of 8 ms, there are occurrences of higher statics reaching up to 20 ms. Figure 15 shows the effect of residual statics on the phase and amplitude after local stacking. The phase of stacked data in red overlays the clean phase (Figure 15b) as predicted by equation 14b. This is a remarkable fact that holds the key to mitigating the effects of residual statics in processing. Figure 15a shows a dramatic attenuation or roll-off of the amplitude at high frequencies that agrees with equation 14b. The steepness of the roll-off increases with increasing standard deviation. Residual statics may be one possible explanation of observation 3 about the significant and progressive loss of higher frequencies after stacking real data. However, it does not explain observations 1 and 2. If data suffer only from residual statics, waveforms remain identical (Figure 13a), whereas low frequencies are virtually untouched; therefore, additional noise types also must be present.

Uniform distribution of residual statics

Let us consider in a similar manner the uniform distribution of residual statics with several ranges $\tau_0 = 4$ ms, $\tau_0 = 8$ ms, and $\tau_0 = 12$ ms. Figure 16 shows the effect of residual statics on the phase and amplitude after local stacking. Whereas in the time domain (Figure 16c), we can see a similar broadening of the wavelet, the details of amplitude and phase spectra are quite different. Similar to the previous case of normal distribution, there also is a roll-off of amplitudes at higher frequencies proportional to the statics ranges. However, amplitude spectra are populated with characteristic notches (Figure 16a) predicted by equation 15b. Before the first notch, the phase of the stacked response agrees with the clean phase (Figure 16b) consistent with equation 15b. However, the phase changes by π after the notch, and this pattern repeats for the subsequent notches. Such characteristic notches are not observed after stacking real data from Figures 3 and 4, suggesting that uniform distribution is not a plausible description for geologic heterogeneity.

Example 2. Random phase perturbations (stack of 1000 traces)

Similarly, let us evaluate the effect of the first type of multiplicative noise represented by random phase perturbations. For brevity, we present only results for the case of normal distribution. Uniform distribution leads to a similar effect. We selected normal distribution as the primary case because the actual phase distribution of the phase for synthetic or real data indicates such a type of distribution as more common (not shown).

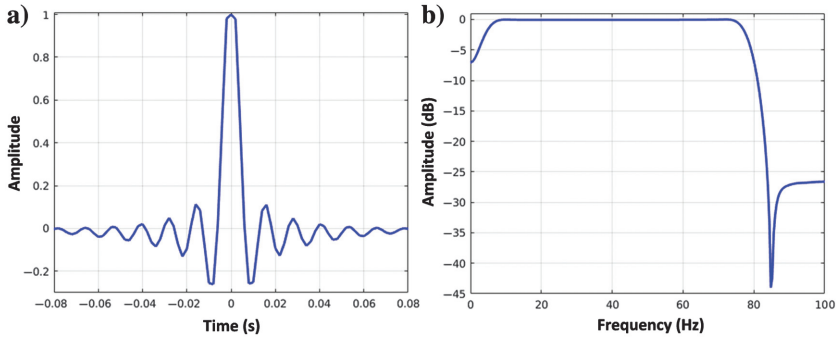

Figure 12. Klauder wavelet used as a clean signal in the synthetic experiments: (a) time-domain representation and (b) amplitude spectrum. Klauder wavelet corresponds to an autocorrelation of the linear sweep 5–80 Hz with appropriate tapers on each side.

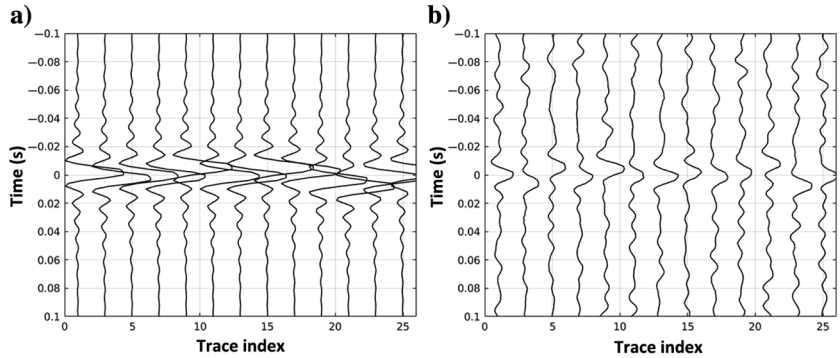

Figure 13. A subset of traces from the ensembles used for numerical examples with different types of multiplicative noise: (a) random timeshifts with a normal distribution ($\sigma_\tau = 4$ ms) and (b) combination of normally distributed random phase perturbations ($\sigma_\varphi = \pi/2$) and timeshifts ($\sigma_\tau = 4$ ms). Synthetic ensemble generated using fixed signal (equation 1) and random realizations of multiplicative noise on each channel. Although (a) exhibits only slight arrival time variation, panel (b) shows severe waveform changes from trace to trace, leading to a reduced coherency.

Normal distribution of phase perturbations

We consider the standard deviations of $\sigma_\varphi = \pi/2$ and $\sigma_\varphi = \pi/1.2$ rad. Figure 17 demonstrates the effect of perturbations on the phase and amplitude of the stacked signal. Similar to previous observations, the stacked phase tracks the phase of the clean signal (Figure 17b). However, amplitude spectra experience a severe constant loss at all frequencies (Figure 17a) because we assume a fixed value of the standard deviation for all frequencies. The magnitude of amplitude bias or loss increases with increasing standard deviation. Phase distortions may explain observations 1 and 2. Indeed, phase distortions change the wavelet shapes and thus reduce coherency significantly (Figure 13b). They also lead to severe amplitude bias or loss after stacking. However, they do not predict amplitude roll-off if we assume a constant standard deviation with frequency. However, suppose that the standard deviation of phase perturbations will increase with a frequency that sounds plausible because higher frequencies become more and more affected by small-scale heterogeneities. In that case, we also could reproduce a similar amplitude roll-off as observed in the case of residual statics (Figure 15a). Therefore, all three observations could be explained. The concept of statics remains a useful simplification. However, we should never forget its limitation, characterized by Meunier (2011), as an "impossibility for such a simplistic propagation model (infinitely low velocity) to account fully for the perturbation of the wavefield associated with the weathered-layer variations." We believe that we can move to a more plausible way to describe near-surface distortions by using phase perturbations. Although still being statistical (as residual statics), it provides a more realistic (wave propagation-based) representation of wavefield perturbations by the near-surface scattering layer. Again, such an upgrade would be consistent with speckle studies in other domains with significant progress achieved.

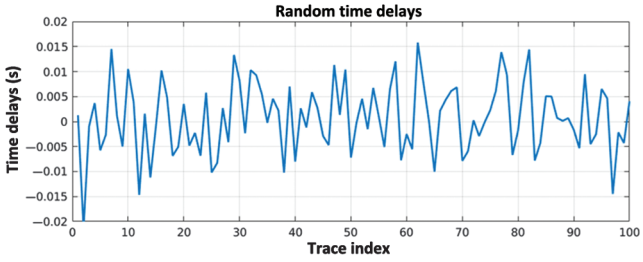

Figure 14. Normally distributed random timeshifts (residual static) as a function of trace index in the ensemble ($\sigma_\tau = 8$ ms).

Example 3. The joint effect of residual statics and random phase perturbations (stack of 1000 traces)

We have established the basic building blocks to understand and explain the real data by analyzing the individual effects of two types of multiplicative noise. We have shown that phase perturbations can explain observations 1 and 2, whereas a residual statics can mimic observation 3. Although we have seen that a more complex form of phase perturbations also could explain observation 3, let us consider one simpler additional case that also consistently explains all observations 1–3 from real data at once. In this example, two types of multiplicative noise act together or superimposed. We stress that the normal distribution of residual statics and phase corrections appears to be the best matching effects seen on real data.

Normally distributed phase fluctuations and residual statics

Let us consider the normal distribution of phase corrections with $\sigma_\varphi = \pi/2$ and residual statics with $\sigma_\tau = 4$ ms. Figure 18 demonstrates the combined action of two types of multiplicative noise on the stacked signal's phase and amplitude. Figure 18c shows how phase fluctuations can distort the input trace shown in green. In the time domain, stacked waveform experiences broadening (Figure 18c). The phase of the stacked response agrees with the phase of the true signal (Figure 18b). Amplitude spectrum experiences substantial loss caused by a combination of downward shift induced by phase perturbations and roll-off of the higher frequencies caused by residual statics (Figure 18a).

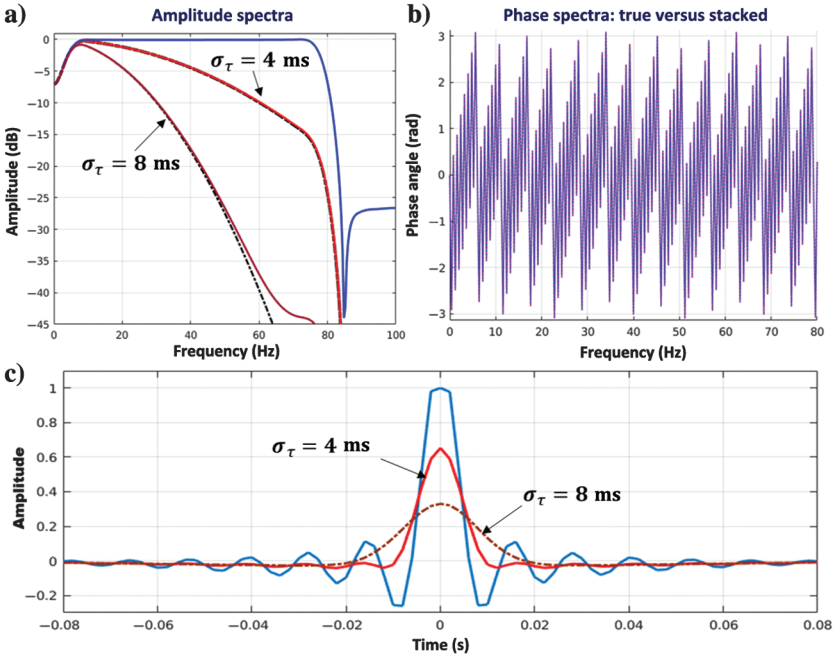

Figure 15. Effect of residual statics on amplitude and phase spectra: (a) amplitude spectra, (b) phase spectra, and (c) time-domain representation. The clean signal is shown in blue; numerically stacked quantities are in red, whereas theoretical predictions are in black: black, red, and blue curves all overlay each other in (b). Panel (a) shows a good match between numerically stacked amplitude spectra in red with theoretical predictions in black. The time-domain representation (c) shows the broadening of the wavelet caused by mis-stacking due to multiplicative noise.

Comparison with real data

Figure 18a can be directly compared with Figures 3c and 4c from real data. Although we are not aiming for a quantitative match, we have fully replicated all observations 1–3, including distorted waveforms, amplitude bias,

and roll-off of amplitudes at higher frequencies. Note that the amplitude bias of phase perturbations (Figures 17a and 18a) replicates the approximate magnitude of the massive 15–30 dB reduction seen in real data (Figures 3c and 4c). We have ignored the effects of random additive noise because stacking perfectly handles such noise without affecting the magnitude of the signal. Data were used in the preceding field examples after a typical processing sequence that was expected to reduce additive noise to manageable levels. Even if we allow the presence of −10 dB additive noise in Figures 3 and 4, local stacking in the presence of additive noise is expected to reduce energy levels by only −5 dB uniformly. In contrast, we see a more massive amplitude reduction of −15 to −20 dB. Although we do not dispute the presence of additive noise, we argue that it is not the main culprit in explaining field observations 1–3. Such conclusions completely agree with studies of acoustic and ultrasonic speckle noise (Damerjian et al., 2014; Goodman, 2020).

The normal distribution of residual statics, as well as phase fluctuations, appears more likely. Numerical experiments with cluttered near-surface layers and real data support the hypothesis of the normal distribution of phase perturbations because histograms of phase deviations are similar to Gaussian-like shapes instead of uniform rectangles (not shown). Likewise, experimental and numerical studies of ultrasonic speckle from a rough water-sand boundary also suggest the Gaussian distribution of phase variations (Hare and Hay, 2020). We have made the simplest assumption of frequency independence of standard deviation for phase perturbations based on initial observations on synthetic and field data. We also have noted that if the standard deviation of phase perturbations would increase with frequency, it also could explain amplitude roll-off at higher frequencies, similar to residual statics. Future studies should examine these assumptions in more detail to fine-tune this understanding.

DISCUSSION AND IMPLICATIONS FOR SEISMIC PROCESSING

Recognizing the essential role of multiplicative random noise in seismic data has important implications. Armed with the new understanding, it is insightful to have a retrospective look at previous seismic practices. Nonsurface-consistent trim statics correction is one known processing step that tries to address small residual timeshifts in prestack data that vary with time. Reilly et al. (2010) describe a 3D dynamic trace alignment procedure similar to trim statics. Remarkably, this procedure also was inspired by challenging offshore seismic data from the Middle East with complex near surface and overburden. They speculate that time-dependent traveltime jitter might be caused by small-to-medium-scale heterogeneities in the velocity model not captured by typical velocity model building. According to their work, addressing such small-scale velocity variations may be equally crucial for time and depth imaging because they remain

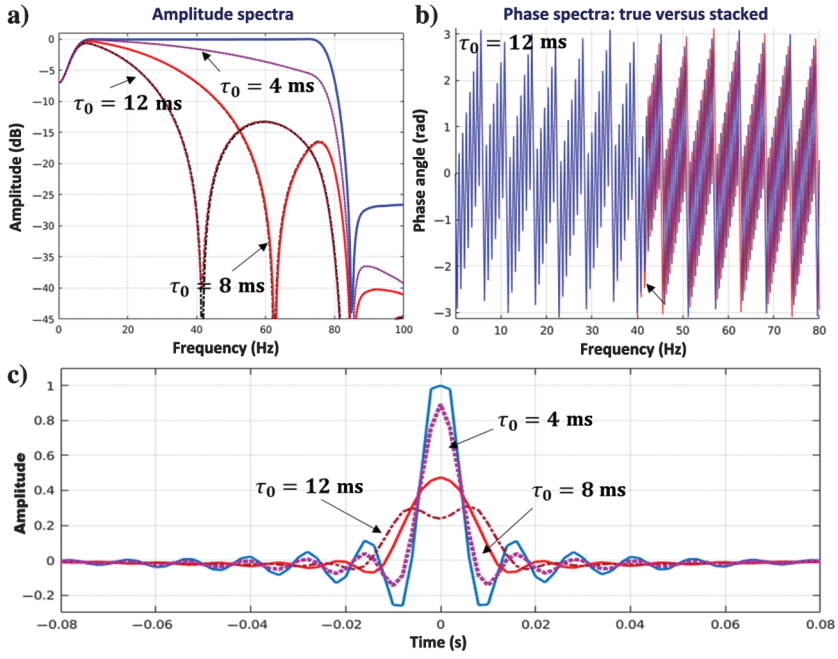

Figure 16. Same as Figure 15 but for uniform distribution of residual statics with different maximum absolute timeshift values (τ_0). Phase spectra for $\tau_0 = 12$ ms only are shown in (b), with a black arrow marking the location of the phase change by π that occurred after the first notch.

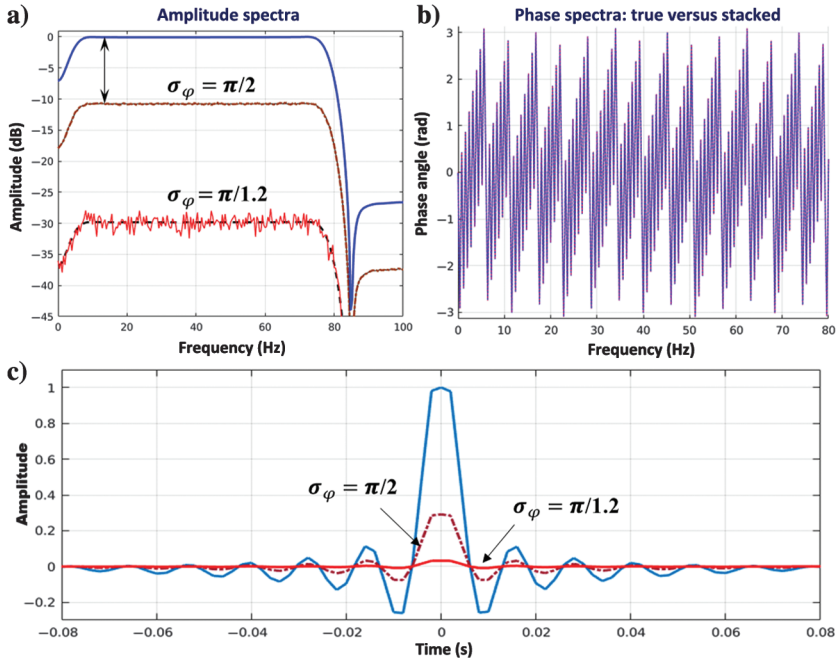

Figure 17. Same as Figure 15 but for normal distribution of phase perturbations with $\sigma_\varphi = \pi/2$ and $\sigma_\varphi = \pi/1.2$ rad.

missed or improperly characterized in the velocity model building process even with advanced techniques such as FWI. However, the statics-based approaches mentioned previously simplistically assume that distortions consist of only small timeshifts but not waveform variations. Also, previous studies did not provide a mathematical model and only described the impact of residual statics on the amplitude (Berni and Roever, 1989), but not the phase. Neklyudov et al. (2017) and Stork (2020) emphasize the role of waveform distortions in land seismic data. They point to the outsized impact of the near-surface layers. Xie et al. (2016) present numerical examples demonstrating that seismic migration suffers a severe loss of focusing when small-scale near-surface heterogeneities are not captured in the velocity model. Khalil and Gulunay (2011) show the robustness and usefulness of local stacking of single-sensor land data as pilots for deriving intraarray statics. Bakulin et al. (2020b, 2020c) suggest phase substitution and phase correction methods that derive an estimate of the clean phase from the beamformed reflected data and show significant improvement in eliminating associated distortions for processing and imaging. Bakulin et al. (2021) further propose seismic time-frequency masking that could use raw amplitude and beamformed amplitude to arrive at an improved estimate of the signal amplitude reducing the loss of higher frequencies. Still, these results lacked a mathematical model and a proper basis for these methods.

The results of this study serve as a theoretical justification explaining that the phase derived from local stacking indeed provides an accurate estimation of the signal phase in the presence of random multiplicative noise caused by near-surface scattering. Remarkably, both types of multiplicative noise in the form of random static shifts and random phase perturbations can be treated using the same approach. In particular, phase perturbations cause waveform distortion and variation that are challenging to fix. Surface-consistent deconvolution is the only process attempting to address the prestack data's variable waveforms, assuming that they can be modeled as deterministic multiplicative distortions. It further relies on the overly simplifying assumptions of surface consistency and time independence that do not capture the essential complexities of 3D wave propagation with small-scale near-surface scattering shown in Figure 1a. The presented mathematical model with random multiplicative noise provides a unified description of residual statics and phase distortions that more accurately capture small-scale scattering effects.

The obtained understanding serves as a foundation for successfully addressing multiplicative speckle noise in seismic processing. Using a random statistical model inspired by studies of optical and ultrasonic speckle (Goodman, 2020), we theoretically justify that the phase derived from local stacking provides an accurate estimation of the signal phase. We believe that such a model has the potential to mitigate many damaging effects of multiplicative seismic noise if we can adequately guess or characterize the distribution of small-scale near-surface heterogeneity. This belief is based on the remarkable progress achieved in addressing the optical and ultrasonic speckle using similar statistical models (Goodman, 2020). Thus, we can still make significant improvements in seismic processing and imaging without ever knowing the exact microscopic details of the near surface.

Why may recognition of speckle noise be so late? As Goodman (2000) points out: "Speckle suppression remains one of the most important unsolved problems of coherent imaging." Speckle noise in optics has been studied since the 1960s, with an initial focus on reflections from rough surfaces having details less than a wavelength (Beckmann, 1962, 1964; Goodman, 1976). The acoustic and ultrasonic speckle came later, starting in the 1980s, recognizing the small-scale volumetric scattering (Abbot and Thurstone, 1979; Fink and Derode, 1998). However, these fields primarily focused on studying and mitigating speckle noise on intensity images at a fixed frequency. In contrast, seismic imaging is always done with broadband signals making speckle noise much harder to recognize among many other effects present in the data. Also, in medical ultrasound, variability between different parts of the population is relatively small compared with vast variations between geologic near-surface heterogeneity present in different parts of the world. In particular, challenging land seismic data, especially from the desert environment, may provide the most substantial evidence of random multiplicative distortions. However, some of that evidence was out of sight because exploration in the desert environment was conducted with large geophone arrays mitigating the effects of multiplicative noise in the field. For example, 72-geophone arrays were used for decades in a desert environment. Currently, acquired data with nine-geophone arrays are significantly more challenging. Single-sensor data in areas with a complex near surface exhibit an ultimate complexity and bring severe processing challenges. The

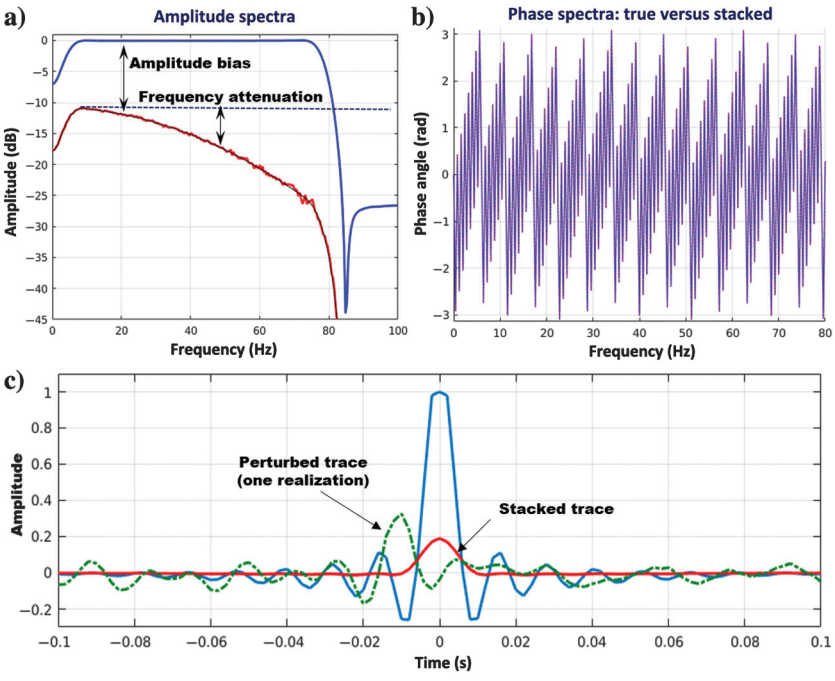

Figure 18. Same as Figure 15 but for normal distribution of phase corrections with $\sigma_\varphi = \pi/2$ and residual statics with $\sigma_\tau = 4$ ms. For illustrative purposes, we also post on (c) a trace from a single channel in green. Note that each ensemble channel is distorted by a different realization of multiplicative noise, as visualized in Figure 13b, showing 25 additional traces from such an ensemble.

DOI:10.1190/geo2021-0830.1

analysis of the latest data with nine-geophone arrays and single sensors leads us to present findings on multiplicative noise.

CONCLUSION

We have carefully analyzed the amplitude and phase spectra's transformation during local stacking of the challenging prestack land seismic data from the desert environment. To explain the key observations from the data, we put forward a seismic trace model with random multiplicative noise describing the effects of small-scale near-surface scattering. We further specified two types of such noise: random phase perturbations and random timeshifts (residual statics). Although not usually described by the multiplicative model, the second type of distortion is well recognized. In contrast, the first type is new and not currently acknowledged in seismic processing. Synthetic modeling confirms that small- and medium-scale near-surface heterogeneities generate random-looking nonsurface-consistent phase perturbations that are different at each frequency. Invoking both types of multiplicative noise, we can semiquantitatively reproduce all three critical observations here from the real data that could not be consistently explained by a conventional model with additive background noise:

1) Even after sophisticated processing, reflections on prestack data remain distorted with low coherency or even untrackable. Such reflection cluttering is not localized in time-space but instead spread over the entire gather in which reflections may be potentially present. In addition, first arrivals also are distorted, making it difficult to pick first breaks or use early arrivals for FWI.
2) After applying local stacking, reflections crop up very clearly; however, the absolute level of amplitude spectra experiences a strong downward bias or loss (-15 to -20 dB or more) across the entire band of frequencies.
3) There is a significant and progressive loss of higher frequencies after local stacking.

Multiplicative noise with random phase perturbations might appear new to the seismic community. However, after closer examination, we suggest that it could be thought of as a seismic version of speckle noise well established in optical, acoustic, and ultrasonic imaging. In a volumetric case, speckle noise occurs when multiple scatterers are present in an elementary volume. Instead of a single ballistic arrival, a wavefield is composed of a superposition of multiple forward-scattered arrivals with adjacent near-ballistic traveltimes. Optical and ultrasonic images with speckle noise exhibit a strong granular imprint that obscures objects under examination. Likewise, seismic prestack data often have substantial amplitude and phase variations even when the underlying reflected signals are expected to be constant or smoothly varying. Specifically, a near-surface layer with small- and medium-scale heterogeneities could be the most likely source of speckle noise, as illustrated by a synthetic example.

Based on this model, we demonstrate that similar to the case of additive noise, stacking remains a useful primary instrument to combat multiplicative noise. Local stacking is particularly useful to mitigate the random nature of speckle noise because the wavepaths involved traverse only a small vicinity of the near surface. Under these conditions, underlying reflection signals are expected to be similar, whereas a fixed local statistical distribution can approximate random multiplicative noise. With this in mind, we have proven that the stacked phase gives an unbiased estimate of the clean signal. This phase estimate's accuracy or standard deviation depends on the number of traces. It requires further studies to find a practical trade-off between accuracy and potential loss of resolution. The recovery of the true signal phase via stacking is the cornerstone to providing a path to mitigate random multiplicative noise in seismic processing and imaging. Such phase recovery was already used in the phase substitution method but without proper justification. With additive noise, stacking estimates the phase and amplitude of the clean signal. With multiplicative noise, stacking provides only an estimate of the clean phase, whereas the recovered amplitude represents a severely distorted version of the signal amplitude. However, providing a simple statistical model describing the anatomy of these distortions could pave the way to mitigating them. Random statistical models proved very productive in addressing the adverse effects of optical and ultrasonic speckle noise. By recognizing seismic speckle, we expect similar progress to mitigate the impact of small-scale scattering on seismic data.

We demonstrate that the proposed model of random multiplicative noise can fully explain all three preceding field observations. Phase perturbations lead to the loss of coherency and amplitude bias or a downward reduction across the entire broadband spectrum, supporting the first and second preceding field observations. In contrast, residual statics only slightly affect amplitudes at low frequencies and instead lead to characteristic amplitude roll-off at medium and higher frequencies explaining the third observation from the field data. When both types of random multiplicative noise act together, we fully replicate the effects seen while stacking complex field data from the desert environment with single sensors or small geophone arrays.

DATA AND MATERIALS AVAILABILITY

Data associated with this research are confidential and cannot be released.

APPENDIX A

MATHEMATICAL EXPRESSIONS FOR AMPLITUDE AND PHASE SPECTRA OF PRESTACK DATA CONSISTING OF MULTIPLE EVENTS

In the frequency domain, each seismic trace $X(\omega)$ can be characterized by its amplitude $|X(\omega)|$ and phase $\varphi_X(\omega)$ spectra uniquely defining the frequency signature of the signal $X(\omega) = |X(\omega)|e^{i\varphi_X(\omega)}$ and its time-domain $x(t)$ representation.

Let the seismic trace $x(t)$ consist of M arrivals. Each arrival has a waveform $f_j(t)$ and corresponding arrival time τ_j:

$$x(t) = \sum_{j=1}^{M} f_j(t - \tau_j). \tag{A-1}$$

In the frequency domain, equation A-1 is rewritten as

$$X(\omega) = \sum_{j=1}^{M} F_j(\omega)e^{i\omega\tau_j} = \sum_{j=1}^{M} |F_j(\omega)|e^{i[\omega\tau_j+\varphi_j(\omega)]}, \tag{A-2}$$

where $|F_j(\omega)|$ and $\varphi_j(\omega)$ are amplitude and phase spectra of jth arrival, respectively.

The following expression gives the power spectrum of the trace (equation A-1):

$$|X(\omega)|^2 = \sum_{n=1}^{M} |F_n(\omega)| e^{i[\omega\tau_n + \varphi_n(\omega)]} \cdot \sum_{m=1}^{M} |F_m(\omega)| e^{-i[\omega\tau_m + \varphi_m(\omega)]}$$
$$= \sum_{j=1}^{M} |F_j(\omega)|^2 + 2\sum_{n=1}^{M-1} |F_n(\omega)| \cdot \sum_{m=n+1}^{M} |F_m(\omega)| \cdot$$
$$\cos\{\omega(\tau_n - \tau_m) + \varphi_n(\omega) - \varphi_m(\omega)\}. \quad \text{(A-3)}$$

A phase spectrum can be derived from the expression:

$$\cos\{\varphi_X(\omega)\} = \frac{\mathrm{Re}\{X(\omega)\}}{|X(\omega)|}$$
$$= \frac{\sum_{j=1}^{M} |F_j(\omega)| \cdot \cos\{\omega\tau_j + \varphi_j(\omega)\}}{|X(\omega)|}. \quad \text{(A-4)}$$

As one can see, the amplitude spectrum depends only on traveltime differences. The phase spectrum is a function of actual traveltimes (Lichman, 1999). In the simplest case, if there is only one arrival ($M = 1$), the amplitude spectrum $|X(\omega)| = |F(\omega)|$, i.e., it does not depend on traveltimes at all. Hence, we conclude that arrival time information of seismic events is encoded in the phase spectrum.

REFERENCES

Abbot, J. G., and F. L. Thurstone, 1979, Acoustic speckle: Theory and experimental analysis: Ultrasonic Imaging, **1**, 303–324, doi: 10.1016/0161-7346(79)90024-5.

Ait-Messaoud, M., M. Boulegroun, A. Gribi, R. Kasmi, M. Touami, B. Anderson, P. Van Baaren, A. El-Emam, G. Rached, A. Laake, S. Pickering, N. Moldoveanu, and A. Özbek, 2005, New dimensions in land seismic technology: Schlumberger Oilfield Review, **17**, 42–53.

Alexandrov, D., A. Bakulin, R. Burnstad, and B. Kashtan, 2015, Improving imaging and repeatability on land using virtual source redatuming with shallow buried receivers: Geophysics, **80**, no. 2, Q15–Q26, doi: 10.1190/geo2014-0373.1.

Bakulin, A., M. Dmitriev, D. Neklyudov, and I. Silvestrov, 2020c, Importance of phase guides from beamformed data for processing multichannel data in highly scattering media: Journal of Acoustical Society of America, **147**, EL447–EL552, doi: 10.1121/10.0001330.

Bakulin, A., I. Silvestrov, M. Dmitriev, D. Neklyudov, M. Protasov, K. Gadylshin, V. Tcheverda, and V. Dolgov, 2018a, Nonlinear beamforming for enhancing prestack data with challenging near surface or overburden: First Break, **36**, 121–126, doi: 10.3997/1365-2397.n0143.

Bakulin, A., D. Neklyudov, and I. Silvestrov, 2020b, Prestack data enhancement with phase corrections in time-frequency domain guided by local multidimensional stacking: Geophysical Prospecting, **68**, 1811–1818, doi: 10.1111/1365-2478.12956.

Bakulin, A., D. Neklyudov, and I. Silvestrov, 2021, Targeted noise removal by seismic time-frequency masking (STFM) and minimum statistics approach: 91st Annual International Meeting, SEG, Expanded Abstracts, 2879–2884, doi: 10.1190/segam2021-3581846.1.

Bakulin, A., I. Silvestrov, and M. Dmitriev, 2019b, Adaptive multiscale processing of challenging 3D seismic data for first-break picking, FWI and imaging: 89th Annual International Meeting, SEG, Expanded Abstracts, 3979–3984, doi: 10.1190/segam2019-3214616.1.

Bakulin, A., I. Silvestrov, M. Dmitriev, D. Neklyudov, M. Protasov, K. Gadylshin, and V. Dolgov, 2020a, Nonlinear beamforming for enhancement of 3D prestack land seismic data: Geophysics, **85**, no. 3, V283–Z13, doi: 10.1190/geo2019-0341.1.

Bakulin, A., P. Golikov, M. Dmitriev, D. Neklyudov, P. Leger, and V. Dolgov, 2018b, Application of supergrouping to enhance 3D prestack seismic data from a desert environment: The Leading Edge, **37**, 200–207, doi: 10.1190/tle37030200.1.

Bakulin, A., I. Silvestrov, and D. Neklyudov, 2019a, Where are the reflections in single-sensor land data? SEG Workshop on New Advances in Seismic Land Data Acquisition.

Baykulov, M., and D. Gajewski, 2009, Prestack seismic data enhancement with partial common-reflection-surface (CRS) stack: Geophysics, **74**, no. 3, V49–V58, doi: 10.1190/1.3106182.

Beckmann, P., 1962, Statistical distribution of the amplitude and phase of a multiply scattered field: Journal of Research of the National Bureau of Standards, Section D: Radio Propagation, **66D**, 231–240, doi: 10.6028/JRES.066D.027.

Beckmann, P., 1964, Rayleigh distribution and its generalizations: Radio Science Journal of Research NBS/USNC-URSI, **68D**, 927–932.

Berkovitch, A., K. Deev, and E. Landa, 2011, How non-hyperbolic Multi-Focusing improves depth imaging: First Break, **29**, 103–111, doi: 10.3997/1365-2397.29.9.53731.

Berni, A. J., and W. L. Roever, 1989, Field array performance: Theoretical study of spatially correlated variations in amplitude coupling and static shift and case study in the Paris Basin: Geophysics, **54**, 451–459, doi: 10.1190/1.1442671.

Blackledget, J. M., 2006, Digital signal processing: Horwood Publishing.

Borcea, L., G. Papanicolaou, and C. Tsogka, 2006, Coherent interferometric imaging in clutter: Geophysics, **71**, no. 4, SI165–SI175, doi: 10.1190/1.2209541.

Buzlukov, V., and E. Landa, 2013, Imaging improvement by prestack signal enhancement: Geophysical Prospecting, **61**, 1150–1158, doi: 10.1111/1365-2478.12047.

Cary, P. W., and G. A. Lorentz, 1993, Four-component surface-consistent deconvolution: Geophysics, **58**, 383–392, doi: 10.1190/1.1443421.

Chan, W. K., and R. R. Stewart, 1994, 3-D *f-k* filtering: CREWES Research Report, **6**, 15.1–15.7.

Damerjian, V., O. Tankyevych, N. Souag, and E. Petit, 2014, Speckle characterization methods in ultrasound images — A review: IRBM, **35**, 202–213, doi: 10.1016/j.irbm.2014.05.003.

Fink, M., and A. Derode, 1998, Correlation length of ultrasonic speckle in anisotropic random media: Application to coherent echo detection: The Journal of the Acoustical Society of America, **103**, 73–82, doi: 10.1121/1.421080.

Goodman, J. W., 1976, Some fundamental properties of speckle: Journal of the Optical Society of America, **66**, 1145–1150, doi: 10.1364/JOSA.66.001145.

Goodman, J. W., 2000, Statistical optics: John Wiley & Sons.

Goodman, J. W., 2007, Speckle phenomena in optics: Theory and applications: Roberts & Company.

Goodman, J. W., 2020, Speckle phenomena in optics: Theory and applications, 2nd ed.: SPIE Press.

Hare, J., and A. E. Hay, 2020, On acoustic reflection from sand-sized water-saturated granular media at MHz frequencies: Measurements, models and the role of speckle: The Journal of the Acoustical Society of America, **148**, 3291–3304, doi: 10.1121/10.0002657.

He, B., X.-B. Xie, H. Ning, Y. He, and B. Chen, 2017, The effect of strong near-surface scattering on the quality of seismic imaging: 87th Annual International Meeting, SEG, Expanded Abstracts, 2715–2720, doi: 10.1190/segam2017-17654529.1.

Ikelle, L. T., S. K. Yung, and F. Daube, 1993, 2-D random media with ellipsoidal autocorrelation functions: Geophysics, **58**, 1359–1372, doi: 10.1190/1.1443518.

Jain, A. K., 1989, Fundamentals of digital image processing: Prentice Hall.

Khalil, A., and N. Gulunay, 2011, Intra array statics (IAS) in the cross-spread domain: 73rd Annual International Conference and Exhibition, EAGE, Extended Abstracts, I037, doi: 10.3997/2214-4609.20149308.

Lichman, E., 1999, Automated phase-based moveout correction: 69th Annual International Meeting, SEG, Expanded Abstracts, 1150–1153, doi: 10.1190/1.1820706.

Liu, C., Y. Liu, B. Yang, D. Wang, and J. Sun, 2006, A 2D multistage median filter to reduce random seismic noise: Geophysics, **71**, no. 5, V105–V110, doi: 10.1190/1.2236003.

Marsden, D., 1993, Static corrections — A review, Part 1: The Leading Edge, **12**, 43–49, doi: 10.1190/1.1436912.

Meunier, J., 1999, 3D geometry, velocity filtering and scattered noise: 69th Annual International Meeting, SEG, Expanded Abstracts, 1216–1219, doi: 10.1190/1.1820725.

Meunier, J., 2011, Seismic acquisition from yesterday to tomorrow: 2011 distinguished instructor short course: SEG, Distinguished Instructor Series N 14.

Moreira, A., P. Prats-Iraola, M. Younis, G. Krieger, I. Hajnsek, and K. Papathanassiou, 2013, A tutorial on synthetic aperture radar: IEEE Geoscience and Remote Sensing Magazine, **1**, 6–43, doi: 10.1109/MGRS.2013.2248301.

Müller, T. M., and S. A. Shapiro, 2001, Most probable seismic pulses in single realizations of two- and three-dimensional random media: Geophysical Journal International, **144**, 83–95, doi: 10.1046/j.1365-246x.2001.00320.x.

Neklyudov, D., A. Bakulin, M. Dmitriev, and I. Silvestrov, 2017, Intraarray statics and phase corrections obtained by beamforming in the short-time Fourier transform domain: Application to supergrouping: 87th Annual International Meeting, SEG, Expanded Abstracts, 4991–4994, doi: 10.1190/segam2017-17585227.1.

Oppenheim, A. V., and J. S. Lim, 1981, The importance of phase in signals: Proceedings of the IEEE, **69**, 529–541, doi: 10.1109/PROC.1981.12022.

Prunty, A. C., and R. K. Snieder, 2017, Demystifying the memory effect: A geometrical approach to understanding speckle correlations: The European Physical Journal Special Topics, **226**, 1445–1455, doi: 10.1140/epjst/e2016-60254-0.

Regone, C., M. Fry, and J. Etgen, 2015, Dense sources vs. dense receivers in the presence of coherent noise: A land modeling study: 85th Annual International Meeting, SEG, Expanded Abstracts, 12–16, doi: 10.1190/segam2015-5833924.1.

Reilly, J. M., A. P. Shatilo, and Z. J. Shevchek, 2010, The case for separate sensor processing: Meeting the imaging challenge in a producing carbonate field in the Middle East: The Leading Edge, **29**, 1240–1249, doi: 10.1190/1.3496914.

Shapiro, S. A., R. Schwarz, and N. Gold, 1996, The effect of random isotropic inhomogeneities on the phase velocity of seismic waves: Geophysical Journal International, **127**, 783–794, doi: 10.1111/j.1365-246X.1996.tb04057.x.

Sivaji, C., O. Nishizawa, G. Kitagawa, and Y. Fukushima, 2002, A physical-model study of the statistics of seismic waveform fluctuations in random heterogeneous media: Geophysical Journal International, **148**, 575–595, doi: 10.1046/j.1365-246x.2002.01606.x.

Stork, C., 2020, How does the thin near surface of the earth produce 10–100 times more noise on land seismic data than on marine data? First Break, **38**, 67–75, doi: 10.3997/1365-2397.fb2020062.

Taner, M. T., and F. Koehler, 1981, Surface consistent corrections: Geophysics, **46**, 17–22, doi: 10.1190/1.1441133.

Ulrych, T. J., S. T. Kaplan, M. D. Sacchi, and E. Galloway, 2007, The essence of phase in seismic data processing and inversion: 77th Annual International Meeting, SEG, Expanded Abstracts, 1765–1769, doi: 10.1190/1.2792834.

Valsesia, D., 2020, You do not need clean images for SAR despeckling with deep learning, https://towardsdatascience.com/you-do-not-need-clean-images-for-sar-despeckling-with-deep-learning-fe9c44350b69, accessed 10 November 2021.

Wells, P. N. T., and M. Halliwell, 1981, Speckle in ultrasonic imaging: Ultrasonics **19**, 225–229, doi: 10.1016/0041-624X(81)90007-X.

Xie, X.-B., H. Ning, and B. Chen, 2016, How scatterings from small-scale near-surface heterogeneities affecting seismic data and the quality of depth image, analysis based on seismic resolution: 76th Annual International Meeting, SEG, Expanded Abstracts, 4278–4282, doi: 10.1190/segam2016-13780223.1.

Biographies and photographs of the authors are not available.

DOI:10.1190/geo2021-0830.1